Available online at www.sciencedirect.com
SCIENCE DIRECT®
Journal of Sound and Vibration 262 (2003) 1091–1112
JOURNAL OF SOUND AND VIBRATION
www.elsevier.com/locate/jsvi

Chaotic rocking behavior of freestanding objects with sliding motion

ManYong Jeong[a,*], Kohei Suzuki[b], Solomon C.S. Yim[c]

[a] *Department of Electronics and Control Engineering, Numazu College of Technology, 3600 Oka Numazu-shi, Shizuoka-ken 410-8501, Japan*

[b] *Department of Mechanical Engineering, Tokyo Metropolitan University, 1-1 Minamiosawa Hachioji-shi, Tokyo 192-0397, Japan*

[c] *Department of Civil Engineering, Oregon State University, Corvallis, OR 97331-2302, USA*

Received 4 May 2000; accepted 1 July 2002

Abstract

This paper examines the influence of effects of sliding on the non-linear rocking response behavior of freestanding rigid objects (blocks) subjected to harmonic horizontal and vertical excitations. It is well known that the rocking responses depend strongly on the impact effect between object and the base, which takes place with abrupt reduction in kinetic energy. In this study, it is shown that the rocking behavior is significantly affected by the presence of the sliding motion. A parametric response analysis is carried out over a range of excitation amplitudes and frequencies. Chaotic responses are observed over a wide response region, particularly for the case of large vertical amplitude excitation with significant sliding motions. The chaotic characteristics are demonstrated using time histories, Poincaré sections, power spectral density and Lyapunov exponents of the rocking responses. The complex chaotic response behavior is illustrated by Poincaré section in the phase space. The distribution of various types of rocking responses and the effects of sliding motion are examined via bifurcation diagrams and examples of typical rocking responses.

1. Introduction

Many offshore equipment on-board vessels and floating production systems are not firmly anchored to their supporting base. Some of these equipment, often modelled as rigid objects (or blocks), in fact, may be considered freestanding. These objects may sometimes be set into rocking and sliding motions due to the wave-induced support motions under severe seas. Damage to these

*Corresponding author. Fax: +559-26-5830.
E-mail address: jeong@ece.numazu.ct.ac.jp (M. Jeong).

0022-460X/03/$ - see front matter
PII: S0022-460X(02)01087-8

equipment due to rocking impact can be costly and may endanger nearby personnel. Thus, an understanding of the rocking and sliding motions is essential for the development of safe operational guidelines, preservation of existing equipment, and improving analysis and design of new ones.

Previous analytical and experimental studies of dynamic behavior of rocking objects have found that rocking motions can be very complex and sensitive. Yim et al. [1] pointed out that the rocking responses of a object may diverge with minute changes in systems parameters or details of excitation. This observation was confirmed by the shake table experimental study by Aslam et al. [2]. They found that for certain combination of system and excitation parameters, the experiments were not repeatable.

Recognizing the complexity of the rocking response and the periodic nature of wave-induced supporting structure motions, researchers in the 1980s focused their studies on simple forms of systems and excitations. Spanos and Koh [3] and Tso and Wong [4] examined the stability of slender objects subjected to horizontal simple harmonic support excitation. Using a piecewise-linear model, they determine the rocking stability of objects and identified safe regions in an amplitude–frequency plane. In addition to harmonic responses, steady state subharmonic responses were detected. Analytical procedures were developed for determining the amplitudes of predominant non-linear modes. Later, Yim and Lin [5], and Lin and Yim [6,7] extended the study to fully non-linear rocking response of rigid objects subjected to combined horizontal and vertical harmonic motions. In addition to harmonic and subharmonic responses, they also found quasi-periodic and chaotic motions. Shenton and Jones [8] further improved the predictive capability of rocking response models by taking into account sliding motions.

This paper shows several basic characteristics of the rocking motion under two-dimensional periodic excitations demonstrated by the response analysis results using non-linear rocking model. Non-linearities of rocking system considered include geometry, the transition of governing equations and the energy dissipation at impact, and sliding between object and base.

2. System considered and analysis procedure

2.1. Rocking and sliding equations

The rocking and sliding rigid object system under horizontal and vertical excitations, $a_h(t)$ and $a_v(t)$, respectively, is shown in Fig. 1, where x, y and θ are the horizontal, vertical and angular displacements, respectively, of the center of mass of the object with respect to the ground (or supporting base). The object is of width B, height H, mass m, the distance between either base corner, O or O', and the center of mass R and the shape angle ψ.

Note that, because it is assumed in this study that there is no loss of contact between the object and the base at any time, the vertical motion of the center of mass, y, relative to the base is a function of the rocking angle, θ, given by

$$y = R\cos(\psi - |\theta|). \tag{1}$$

However, we will continue to use the variable y in some equations for convenience of expression and interpretation. The reaction forces between the base of the object and the base surface in the

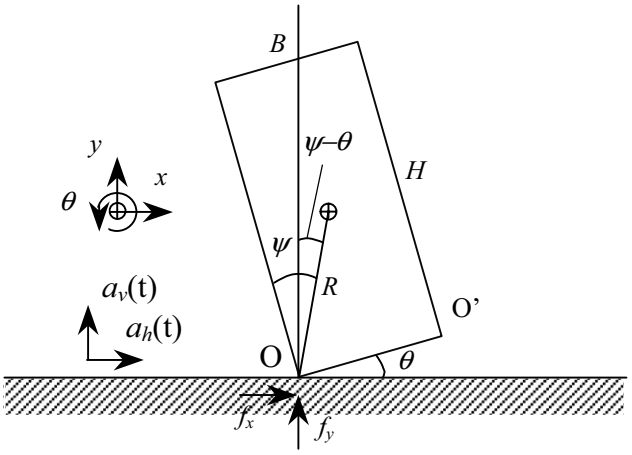

Fig. 1. Rocking rigid block system.

horizontal and vertical directions, f_x and f_y, respectively, are given by

$$f_x = m\ddot{x} + ma_h(t), \tag{2}$$

$$f_y = m\ddot{y} + mg + ma_v(t). \tag{3}$$

Rocking motion is initiated (at time t) when the following condition is satisfied:

$$a_h(t) > \frac{B}{H}\{g + a_v(t)\}, \tag{4}$$

where g is acceleration due to gravity.

Similarly, sliding motion will occur when the following condition is satisfied:

$$\mu_s < \frac{\ddot{x} + a_h(t)}{\ddot{y} + g + a_v(t)}, \tag{5}$$

where μ_s, is the static friction coefficient between the object and the base. When sliding or sliding and rocking (sliding/rocking) occurs, the relationship between the horizontal and vertical reaction forces and the kinetic friction coefficient, μ_k, between the object and the base is as follows:

$$m\{\ddot{x} + a_h(t)\} = -S(\dot{x}_o)m\mu_k\{\ddot{y} + g + a_v(t)\}. \tag{6}$$

The governing equation of motion about the rotation centers of O and O' is presented by

$$I_o\ddot{\theta} = mR\{\ddot{y} + g + a_v(t)\}\{S(\theta)\sin(\psi - |\theta|) + S(\dot{x}_o)\mu_k\cos(\psi - |\theta|)\}, \tag{7}$$

where I_o is the moment of inertia of the object about its edges given by

$$I_o = \frac{4mR^2}{3} \tag{8}$$

and the alternative equations are defined by the signum function, $S(a)$, where

$$S(a) = 1(a > 0), \tag{9}$$

$$S(a) = -1(a < 0). \tag{10}$$

Introducing the following normalization $\Theta = \theta/\psi$, $\dot{\Theta}_p = \dot{\Theta}/p$, $\tau = pt$, $\Omega = \omega/p$, $X = x/R$ and $X_o = x_o/R$, where

$$p^2 = \frac{mgR}{I_o} = \frac{3g}{4R}, \tag{11}$$

the (non-dimensionalized) rocking and sliding equations can be expressed as

$$\ddot{\Theta} + p^2 f_1(\Theta, \dot{\Theta}_p, \dot{X}) = 0, \tag{12}$$

$$\ddot{X} + p^2 f_2(\Theta, \dot{\Theta}_p, \dot{X}) = -\frac{a_h(\tau)}{R}, \tag{13}$$

in which $f_1(\Theta, \dot{\Theta}_p, \dot{X})$ and $f_2(\Theta, \dot{\Theta}_p, \dot{X})$ are given as follows:

$$f_1(\Theta, \dot{\Theta}_p, \dot{X}) = \frac{S(\Theta)\{\sin\psi(1-|\Theta|) + S(\Theta)S(\dot{x}_o)\mu_k \cos\psi(1-|\Theta|)\}\{1 + (a_v(\tau)/g) - \gamma\cos\psi(1-|\Theta|)\dot{\Theta}_p^2\}}{\{1 + \gamma\sin^2\psi(1-|\Theta|) + \gamma S(\Theta)S(\dot{X}_o)\mu_k \cos\psi(1-|\Theta|)\sin\psi(1-|\Theta|)\}}. \tag{14}$$

$$f_2(\Theta, \dot{\Theta}_p, \dot{X}) = \frac{S(\Theta)S(\dot{x}_o)\mu_k \cos\psi(1-|\Theta|)\{1 + (a_v(\tau)/g) - \gamma\cos\psi(1-|\Theta|)\dot{\Theta}_p^2\}}{\gamma\{1 + \gamma\sin^2\psi(1-|\Theta|) + \gamma S(\Theta)S(\dot{X}_o)\mu_k \cos\psi(1-|\Theta|)\sin\psi(1-|\Theta|)\}}, \tag{15}$$

where

$$\gamma = \frac{mR^2}{I_o}. \tag{16}$$

The horizontal and vertical base excitation are, respectively, assumed by

$$a_h(\tau) = A_h\psi g \sin(\Omega\tau + \Phi), \tag{17}$$

$$a_v(\tau) = A_v\psi g \sin(\Omega\tau + \Phi). \tag{18}$$

The non-dimensionalized horizontal displacement X_o and velocity $\dot{X}_o$ of the object edge are expressed as follows:

$$X_o = X - S(\Theta)R\sin\psi(1-|\Theta|), \tag{19}$$

$$\dot{X}_o = \dot{X} + R\cos\psi(1-|\Theta|). \tag{20}$$

2.2. Impact between object and base

Impact between the object and the base is highly non-linear and needs to be carefully modelled. Energy dissipation at impact without sliding motion is constant and that depends on object shape (i.e., slenderness ratio). In the literature, energy dissipation is often characterized by the restitution coefficient, e, as described in Yim et al. [1]. However, when sliding motion occurs, the energy dissipation is a function of the magnitude of the horizontal sliding motion. Using the principle of impulse and momentum, an impact model was established by Shenton [8]. The effects of sliding motion for impact were illustrated in our previous studies [9–11]. When the object goes toward to impact from rocking and rocking and sliding (rock/slide) motion at impact, the normalized post-impact velocities of the mass center, the scalar components $\dot{X}_2$, $\dot{Y}_2$ and $\dot{\Theta}_2$, are expressed in terms

of the pre-impact velocities $\dot{X}_1$, $\dot{Y}_1$ and $\dot{\Theta}_1$ as follows:

$$\dot{X}_2 = -\frac{H\delta_i}{2}\dot{\Theta}_1, \tag{21}$$

$$\dot{Y}_2 = -S(\Theta_1)\frac{B}{2}(\delta_i + 2e)\dot{\Theta}_1, \tag{22}$$

$$\dot{\Theta}_2 = \delta_i\dot{\Theta}_1, \tag{23}$$

in which the energy dissipation rate δ_i is defined as

$$\delta_i = 1 - \tfrac{3}{4}(1 + \lambda_x)\cos^2\psi - \tfrac{3}{2}(1 + e)\sin^2\psi \tag{24}$$

and the rate of horizontal velocity and angular velocity λ_x and the restitution coefficient e, respectively, are given by

$$\lambda_x = \frac{2\dot{X}_1}{H\dot{\Theta}_1}, \tag{25}$$

$$e = 1 - \tfrac{3}{2}\sin^2\psi. \tag{26}$$

Subscripts 1 and 2 refer to pre- and post-impact quantities, respectively, and subscript i refers to the impact corner. For pure rocking motion (no sliding) at pre-impact, the rate λ_x is -1. During impact, the condition of sliding occurrence is given by

$$\bar{\mu}_s > \left|\frac{H(\delta_i + \lambda_x)}{B(1 + \delta_i + 2e)}\right|, \tag{27}$$

where $\bar{\mu}_s$ is the static friction coefficient between object and base during impact. For the case of the object with rotation and sliding, the normalized post-impact velocities are expressed by

$$\dot{X}_2 = \dot{X}_1 + S(\Theta_1)S(\dot{X}_{i2})\bar{\mu}_k\frac{B\psi}{2R}(1 + \bar{\delta}_i + 2e)\dot{\Theta}_1, \tag{28}$$

$$\dot{Y}_2 = -S(\Theta_1)\frac{B}{2}(\bar{\delta}_i + 2e)\dot{\Theta}_1, \tag{29}$$

$$\dot{\Theta}_2 = \bar{\delta}_i\dot{\Theta}_1, \tag{30}$$

where $\bar{\mu}_k$ is the kinetic friction coefficient at impact and the normalized energy dissipation $\bar{\delta}_i$ in the case of with sliding is given by

$$\bar{\delta}_i = \frac{1 - 3\left\{1 - S(\Theta_1)S(\dot{X}_{i2})\bar{\mu}_k\dfrac{H}{B}\right\}(1 + 2e)\sin^2\psi}{1 + 3\left\{1 - S(\Theta_1)S(\dot{X}_{i2})\bar{\mu}_k\dfrac{H}{B}\right\}\sin^2\psi}. \tag{31}$$

In the previous expressions, $S(\Theta_1)$ denotes the pre-impact sign of Θ, $S(\dot{X}_{i2})$ the sign of post-impact velocity of the impacting corner in the horizontal direction.

2.3. Numerical procedure

Using a variable time-step Runge–Kutta method, the rocking and sliding responses of the rigid object system are simulated numerically to investigate its chaotic characteristics. The standard normalized sampling time of the numerical integration is 0.004. At time of impact or initiation of sliding (with corresponding equation transitions), the integration time-step is iteratively reduced by a factor of 10 each time until normalized angular displacement becomes sufficiently small (10^{-6} or less). When contact is reached (rotation angle equals zero), the transition of the rocking equations is carried out by adopting Eqs. (23) and (31) according to kinetic energy dissipation at impact. An accurate rocking response analysis procedure (see Appendix A) has been developed and implemented to obtain accurate numerical results. The algorithm includes two major processes—rotation and impact. The rotation process determines if sliding occurs with rotation motion by formula (5) and solves the simultaneous equations of (12) and (13) by the Runge–Kutta method. The impact process determines the point of normalized zero angular displacement, calculates the post-impact velocity by formula (24) or (30) and then exchanges the signum function $S(\Theta)$ in the rocking equation. In this study, unless otherwise stated, representative object width of $B = 1\,\mathrm{m}$ and height $H = 4\,\mathrm{m}$ and the associated restitution coefficient e based on Eq. (26) are employed. The following five methods of chaotic analysis are used to study the rocking and sliding responses. First, bifurcation diagrams are created by plotting the normalized angular displacement sampled at periodic points in the rocking response for 50 000 points (after steady state has been achieved). The diagram shows variations in periodicity of the response as a function of excitation amplitude. The bifurcation diagrams are constructed with sampling amplitude increments of 0.05 for horizontal excitation only, and 0.02 vertical excitation with fixed horizontal excitation amplitude. Blanks (of gaps) between amplitude increments represent overturning of the object. Second, time histories of selected individual responses are plotted to demonstrate response characteristic. Third, power spectral densities of the rocking responses are constructed by using time history of 3000–7096. These density functions are employed to examine the periodicity of responses. Periodic, quasi-periodic, and chaotic responses have a single dominant frequency, a finite number of incommensurate frequencies, and an infinite number of frequencies (i.e., a wideband spectrum), respectively. Fourth, Poincaré sections are constructed by the strobe points in the phase space for the rocking response sampled at periodic points of the horizontal (and vertical) excitations. The diagram appears as a strange attractor in a case of the chaotic response, and one or more fixed points in a case of the periodic response. Fifth, the largest Lyapunov exponent, which is a quantitative measure of the divergence rate of nearby trajectories in phase space, is also computed. The exponents of chaotic responses are positive, whereas those of quasi-periodic responses are zero, and periodic are negative.

3. Undamped rocking responses

The undamped rocking responses under horizontal excitation only and combined horizontal and vertical excitations are examined in this section.

3.1. Horizontal excitation only

In order to investigate the basic behavior of the rocking system, responses of the undamped case, which assumes no kinetic energy dissipation at impact, is first considered. The rocking system behavior characteristics of this system give the basic concept and significant information on understanding the non-linear characteristics of damped rocking system. For slender rigid objects, Yim et al. [5] performed a linearized stability analysis based on eigenvalues, and found that there exists no stable periodic response for any combinations of system and excitation parameters. Only quasi-periodic and chaotic responses can be stable. This analytical prediction of the response behavior of undamped systems is confirmed based on numerical results obtained in this study even for non-slender (i.e., non-linear system equations) rocking objects. As shown in Fig. 2, there is no stable periodic response, only quasi-periodic, chaotic and overturning responses exist. The bifurcation diagram also shows that the maximum response amplitude increases, and overturning is more likely to occur with increasing excitation amplitude. In fact, for normalized horizontal excitation amplitude A_h less than about 3.8, the response amplitude is less than 0.1. However, it appears that overturning would likely occur for A_h exceeding 10. A typical example of chaotic responses of the undamped rocking rigid object system subjected to horizontal excitation only is shown in Fig. 3. Observe that the chaotic rocking response has an aperiodic time history (Fig. 3a) and its power spectral density (Fig. 3b) forms an infinite number of frequencies. The Poincaré section (Fig. 3c) clearly demonstrates that the response is chaotic. Note that the rocking amplitude is restricted to around 0.1.

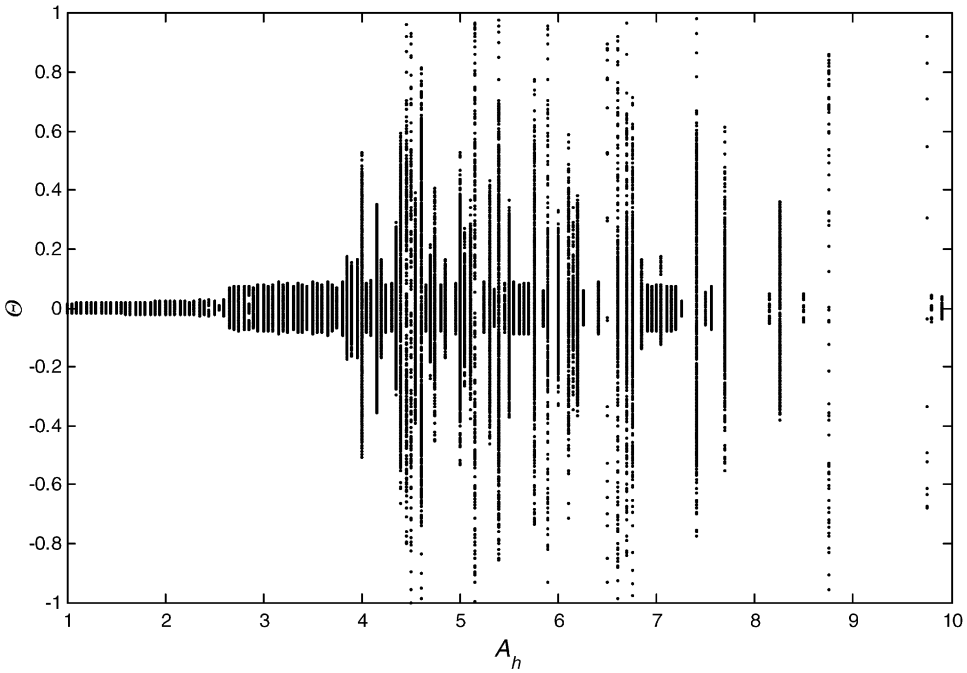

Fig. 2. Bifurcation diagram of undamped rocking responses subjected to horizontal excitation only ($\Omega_h = 15.708$, $e = 1$).

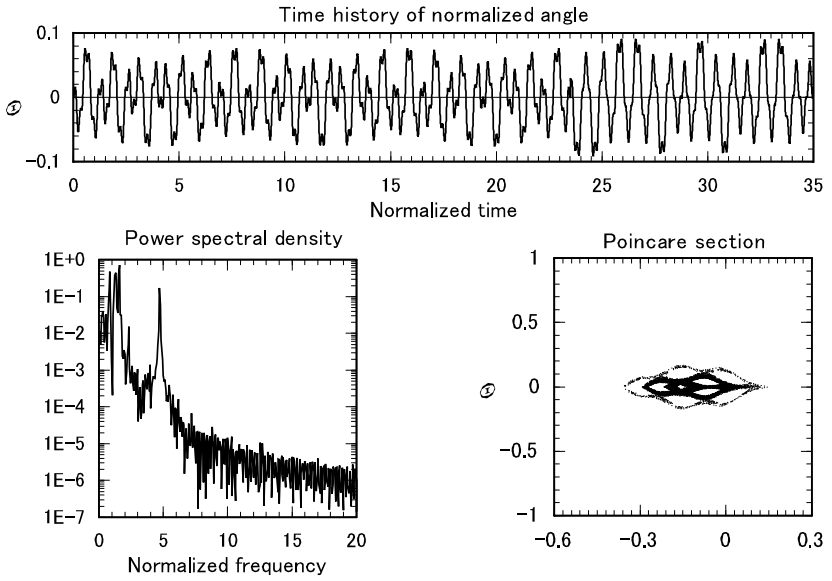

Fig. 3. Typical chaotic response of an undamped rocking system subjected to horizontal excitation only ($\Omega_h = 15.708$, $A_h = 3.958$, $e = 1$).

Fig. 4, shows a typical example of overturning responses of the undamped rocking response. As shown in Figs. 4a, d and e, the response shape varies with the time change and the trajectory increases or decreases in size. It is interesting to observe that prior to overturning, the time history (Fig. 4a), and the power spectral density (Fig. 4b) are similar to that of the stable chaotic response. This is expected because the two systems have identical parameters except for a unit difference in the fifth significant figure in the horizontal excitations. However, asymptotically, the Poincaré section shows the prevalent of large-amplitude responses leading to overturning. This large-amplitude response prior to overturning is shown in Fig. 4e. These two responses show that the undamped rocking response can be very sensitive to small variations in the excitation parameters.

3.2. Horizontal and vertical excitations

The effects of the presence of vertical excitation on rocking response are examined here using a system with fixed horizontal excitation. As shown in Fig. 2, when the rigid rocking object is subjected to horizontal excitation only, for $A_h = 3$, the Poincaré points are restricted to the narrow region less than $\Theta = 0.1$. However, as shown in the bifurcation diagram in Fig. 5, the attraction domain of the responses becomes larger when the vertical excitation is present. It can be observed that the sensitivity of the response to excitation amplitude variations increases compared to the case of horizontal excitation only and the transition of rocking response amplitude versus vertical excitation amplitude becomes more rapid. Responses in the region of vertical amplitude $A_v = 2$ or higher indicate overturning for all cases.

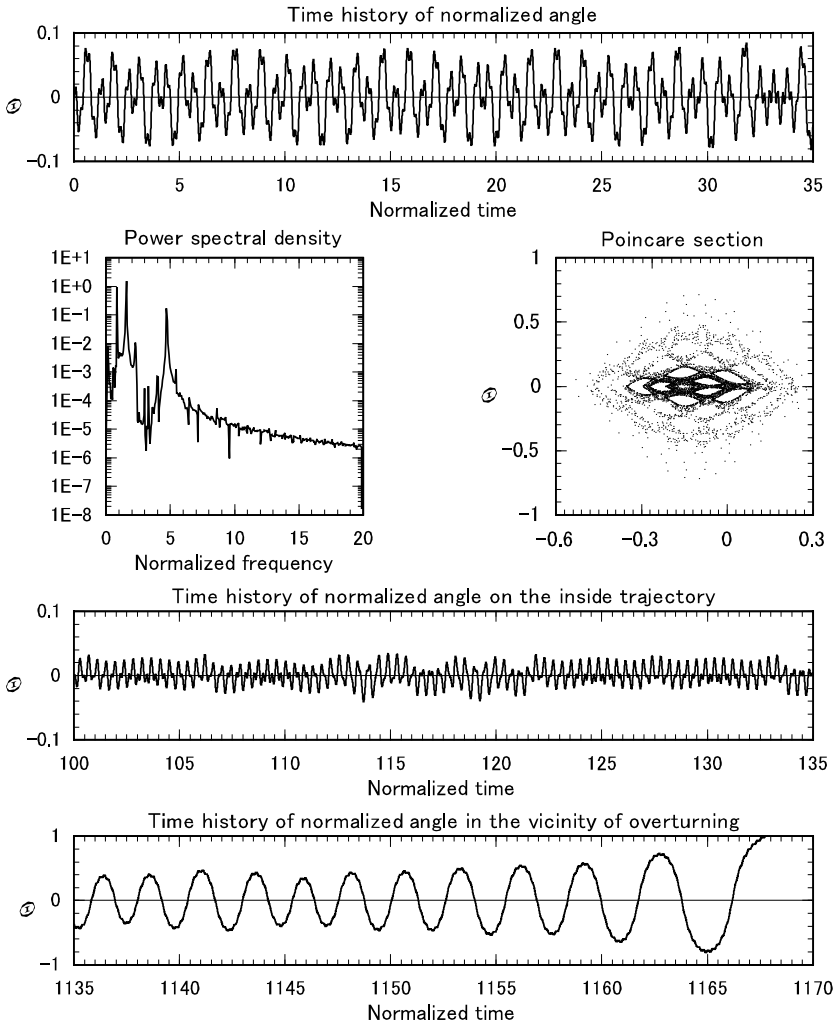

Fig. 4. Typical overturning response of an undamped rocking system subjected to horizontal excitation only ($\Omega_h = 15.708$, $A_h = 3.957$, $e = 1$).

Typical examples of undamped rocking responses of the rigid object subjected to horizontal and vertical harmonic excitations are show in Figs. 6 and 7. As shown in (a) and (b) of these figures, the rocking responses have aperiodic time histories and its power spectral densities contain an infinite number of frequencies. As shown in Fig. 6c, under horizontal and vertical periodic excitations, the Poincaré sections show a strange attractor of asymmetric structure. The example Poincaré sections shown in Fig. 7 show the rocking response diverges to the whole of phase space, leading to overturning. The largest Lyapunov exponents for these rocking responses are 1.1 and 0.31, respectively.

When vertical excitation is introduced in combination with horizontal excitation, the attractor of the rocking response system becomes divergence in the phase space, as a result, the possibility

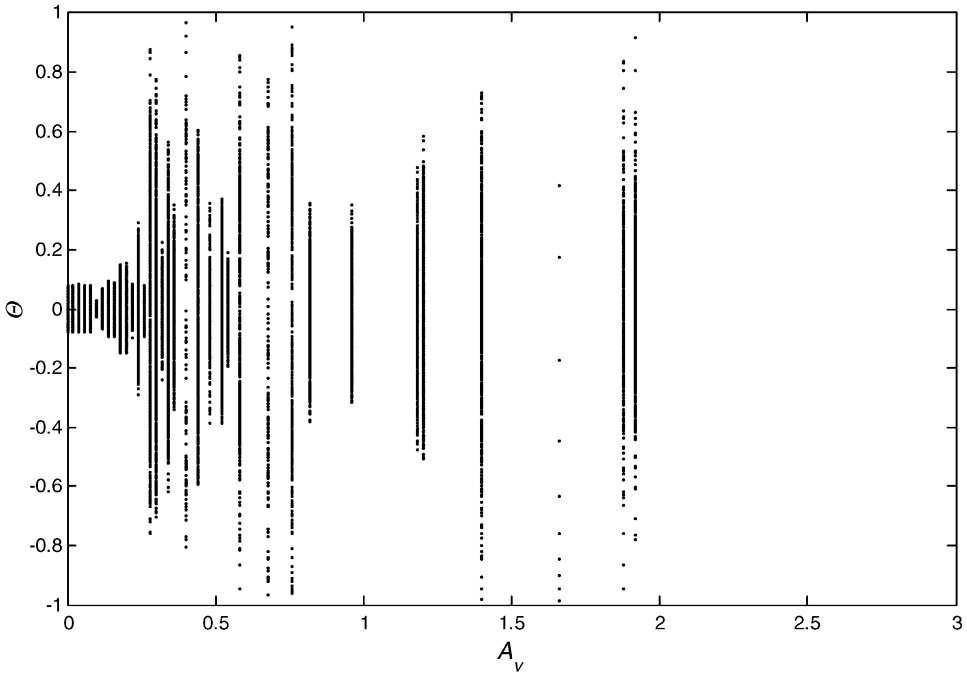

Fig. 5. Bifurcation diagram showing the effects of vertical excitation on undamped rocking response ($\Omega_h = \Omega_v = 15.807$, $A_h = 3.0$, $e = 1$).

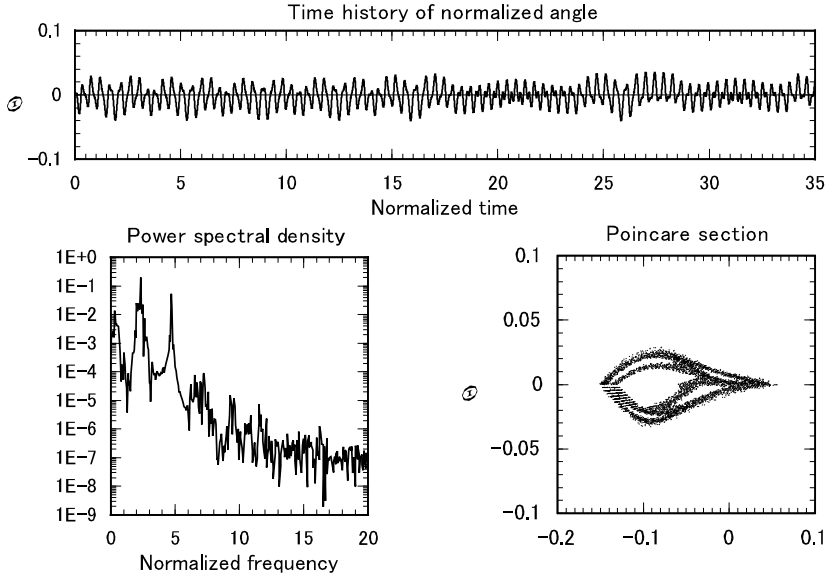

Fig. 6. Example of stable undamped rocking response under horizontal and vertical excitations ($\Omega_h = \Omega_v = 15.708$, $A_h = 2.0$, $A_v = 0.15$, $e = 1$).

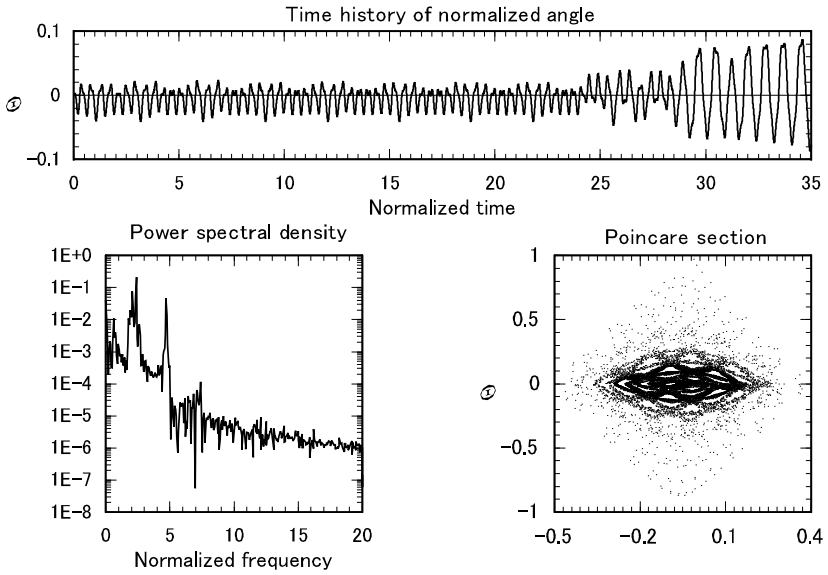

Fig. 7. Example of undamped overturning rocking response under horizontal and vertical excitations ($\Omega_h = \Omega_v = 15.708$, $A_h = 2.0$, $A_v = 0.35$, $e = 1$).

of object overturning is increased. In this case, the bifurcation diagram shows a lot wider spread than that of horizontal excitation only, extending to the whole of the rocking domain. The response behavior by horizontal and vertical excitation is also more sensitive to variations of system or excitation parameters.

4. Damped rocking responses

The model employed in the analysis presented in the above section does not include energy dissipation. However, in real freestanding rocking rigid objects, energy is dissipated at impact as the bottom of the object recontacts the supporting base. This energy dissipation, which is an important system characteristics, is represented by the restitution coefficient, e. In general, a smaller restitution coefficient (more energy dissipation per impact) makes the freestanding object more stable against overturning. However, it is difficult to determine the value of e for seismic design because of its dependency on the mass distribution of the object and the slenderness ratio. In this study, the rigid objects are assumed rectangular and the masses uniformly distributed, hence the restitution coefficient e can be determined using Eq. (26).

4.1. Horizontal excitation only

For the rigid rocking system considered in Fig. 2, but now with a restitution coefficient of $e = 0.912$, subjected to horizontal harmonic excitation with frequency $\Omega_h = 15.708$ and amplitude $A_h = 1-10$, the rocking response becomes periodic motions (harmonics, $\frac{1}{3}$ and $\frac{1}{4}$

subharmonics) only (see Fig. 8a). Quasi-periodic, chaotic and overturning motions shown in Fig. 2 have all been eliminated, thus showing the stabilizing effect of damping. Fig. 8b shows the bifurcation diagram of the same rocking system for the horizontal to excitation frequency $\Omega_h = 10.0$. Note that except for the difference in response amplitudes, the bifurcation diagrams (Fig. 8a and b) exhibit similar behaviors, namely, both show periodic responses of (1,1) mode, transition to (1,3) and (1,4) modes, and back to periodic (1,1) mode as excitation amplitude increases. The large rocking responses for the lower excitation frequency is due to the increased in excitation displacement amplitude, which is inversely proportional to the excitation frequency squared.

4.2. Horizontal and vertical excitations

In this section, the effects of vertical excitation on the non-linear rocking response characteristics are examined. Except for the introduction of vertical acceleration, identical system and excitation parameters as those selected in Sections 3 and 4.1 (i.e., $B = 1\,\text{m}$, $H = 4\,\text{m}$, $e = 0.912$ and $\Omega_h =$ 15.708 or 10) are retained for comparison purpose. The vertical excitation amplitude employed here varies from 0 to 3, while the normalized horizontal acceleration excitation is fixed at 3.0, thus keeping the vertical excitation is no larger than that of the horizontal. We have selected the simple case of horizontal and vertical harmonic excitations being in phase, thus the excitation amplitudes are always in a constant proportion. Fig. 9a and b show the bifurcation diagrams of the rocking responses, with excitation parameters $\Omega_h = \Omega_v = 15.708$ and $\Omega_h = \Omega_v = 10$, respectively. The sampling amplitude spacing of the vertical excitation is 0.02, and blanks in the diagram indicate overturning of the rigid object. As shown in these bifurcation diagrams, the rocking responses transit from harmonics ((1,1) mode) with no vertical excitation ($A_v = 0$), to subharmonics ((1,2) mode), to quasi-periodic, and eventually to chaotic (and overturning for the case of $\Omega_h = \Omega_v = 10$) as the vertical excitation amplitude increases. Thus, the presence of vertical excitation can induce complex responses. Note that there is no overturning for the larger excitation frequency case (Fig. 9a) with overturning occurs for the smaller excitation frequency (Fig. 9b). As explained in the above section, the displacement of response becomes larger for lower excitation frequency (larger displacement amplitude for a given acceleration amplitude) case the same way as the case of the responses to horizontal excitation only. Therefore, the possibility of overturning increases with decreasing of excitation frequency.

Fig. 10 shows the time history, power spectral density and Poincaré section of an example of chaotic rocking response under both horizontal and vertical excitations. It is characterized by a unique asymmetrical shape about the origin and whirling in the anticlockwise direction. Compared to the undamped case (Fig. 6), the boundary of the attractor is not as clearly defined. The characteristic shape of the chaotic attractor of the rocking response is maintained for various excitation parameters. The largest Lyapunov exponent for the response was 1.04.

5. Rocking responses with sliding

For practical freestanding rocking objects, depending on the friction coefficient between the object and the supporting base, sliding may occur. The probability of sliding happening also

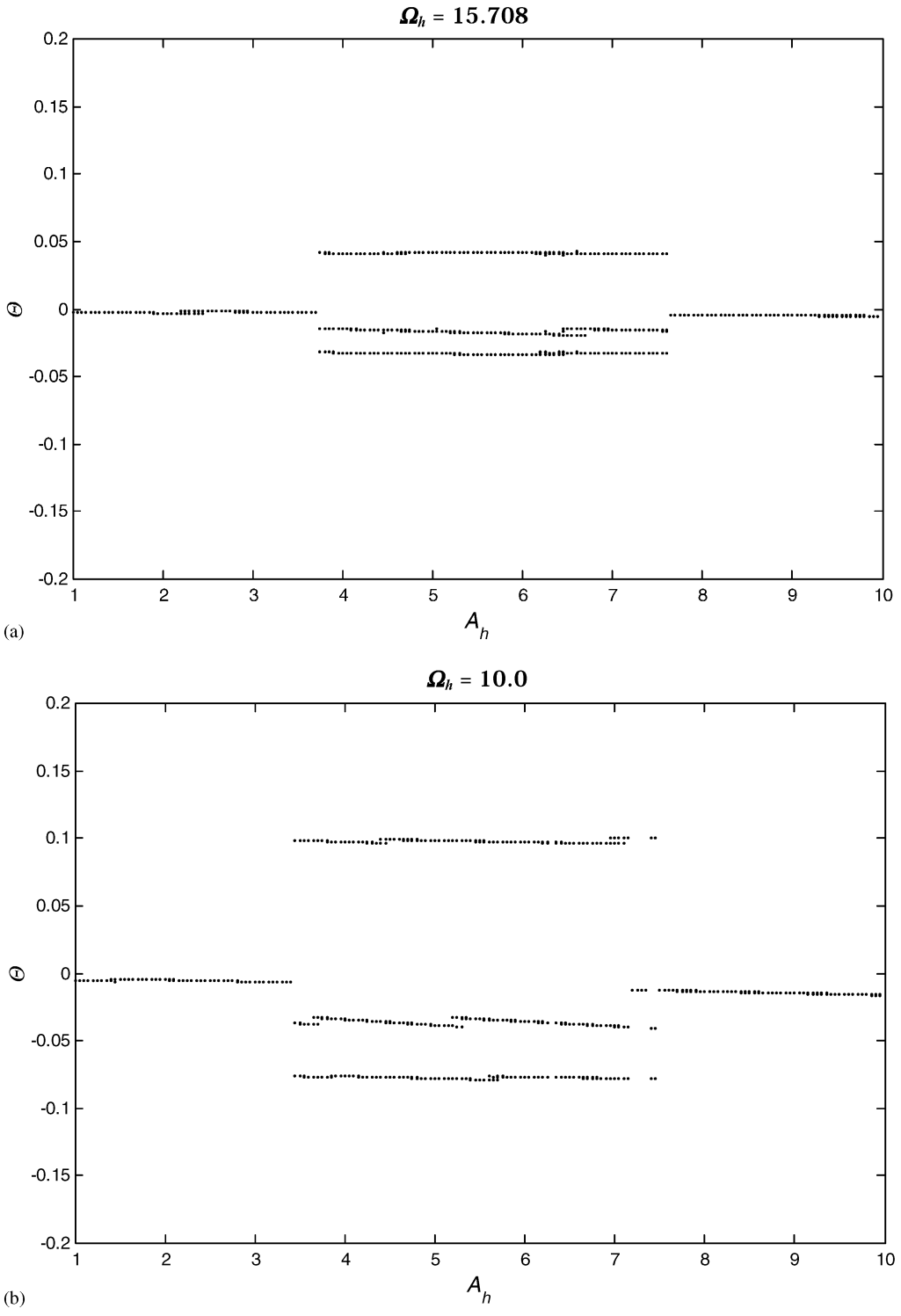

Fig. 8. Bifurcation diagram of damped rocking responses showing the influence of excitation frequency on rocking responses ($e = 0.912$).

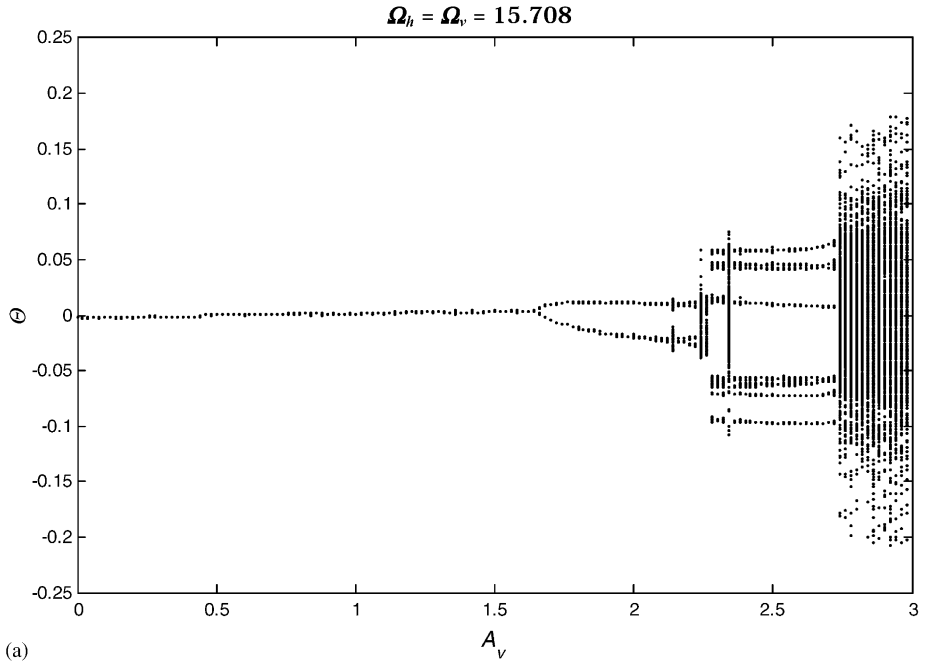

(a)

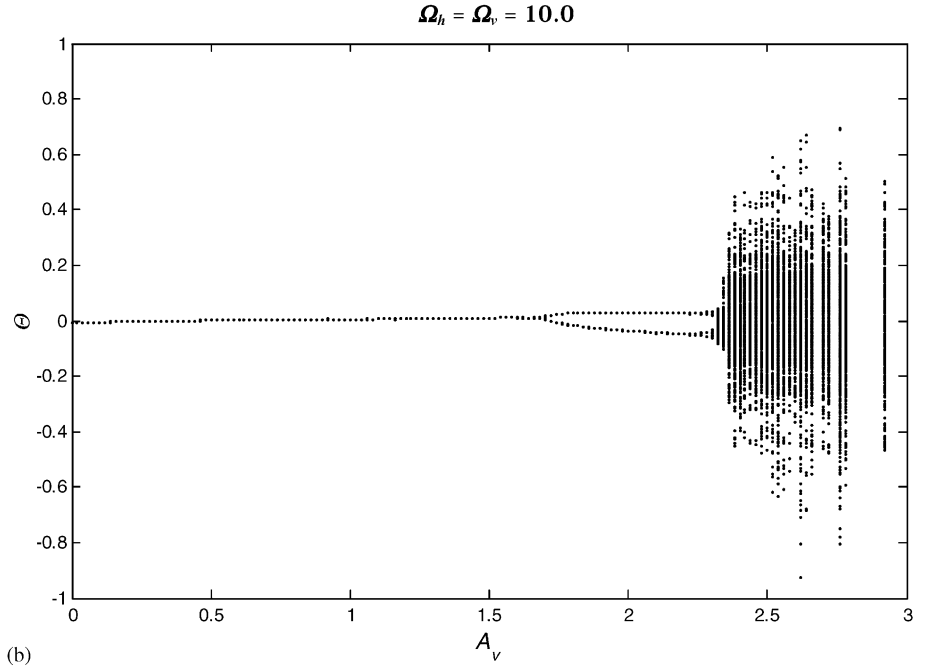

(b)

Fig. 9. Bifurcation diagram showing the effects of excitation frequency on rocking responses under horizontal and vertical excitations ($A_h = 3.0$, $e = 0.912$).

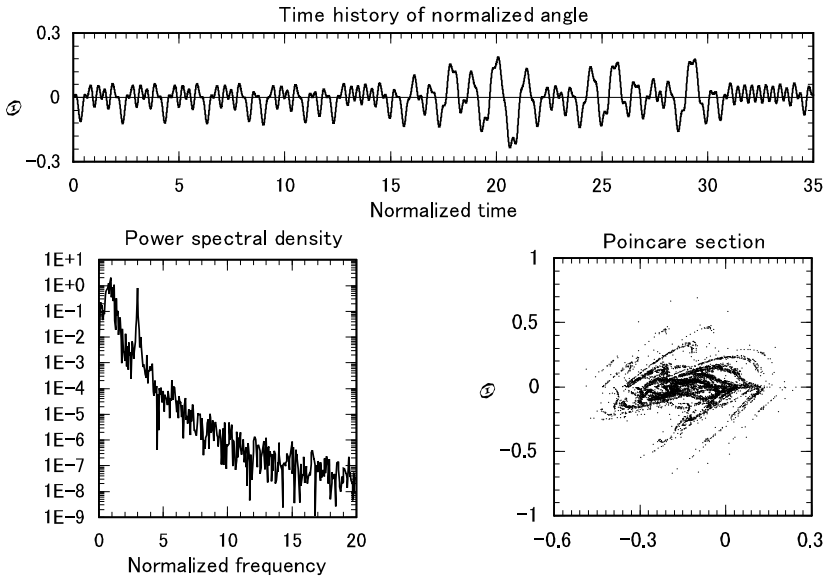

Fig. 10. Typical chaotic damped rocking response to horizontal and vertical excitations ($\Omega_h = \Omega_v = 10.0$, $A_h = 3.0$, $A_v = 2.5$, $e = 0.912$).

increases with decreasing slenderness ratio (which is the case for a wide range of rigid objects). Thus it is essential to take sliding into account in analyzing the rocking response. In this study, the influence of sliding on the non-linear response characteristics of the rocking motion are examined for two cases, with static and kinetic friction coefficients of 0.35 and 0.3, and 0.4 and 0.35, respectively.

5.1. Horizontal excitation only

Fig. 11 shows the bifurcation diagram of the rocking response of the rigid object subjected to a fixed horizontal excitation frequency ($\Omega_h = 10.0$), and horizontal acceleration amplitude $A_h = 1-10$. The static and kinetic friction coefficients, at impact and rocking, are assumed $\mu_s = \bar{\mu}_s = 0.35$, and $\mu_k = \bar{\mu}_k = 0.3$, respectively. The restitution coefficient e is set at 0.912. Note that the response becomes chaotic for several excitation amplitudes when the system is permitted to slide (cf. Fig. 8b only harmonics and subharmonics occurs when sliding is not permitted). In addition, in the excitation amplitude region between 3.5–7.7, sliding suppresses the occurrence of the $\frac{1}{3}$ subharmonic (i.e., (1,3) mode) and the responses are either harmonic or chaotic. An example of the rocking response with sliding, shown in Fig. 12, shows that with sliding, the response becomes chaotic (cf. Fig. 8b, which shows the steady state response to be $\frac{1}{3}$ subharmonic when sliding is not permitted). As shown in the time history, Fig. 12a, initially (0–35 normalized time) the response appears periodic. However, the response eventually becomes chaotic response (Fig. 12c, d and e). Based on our numerical study, the rocking response has a strong sensitive dependence

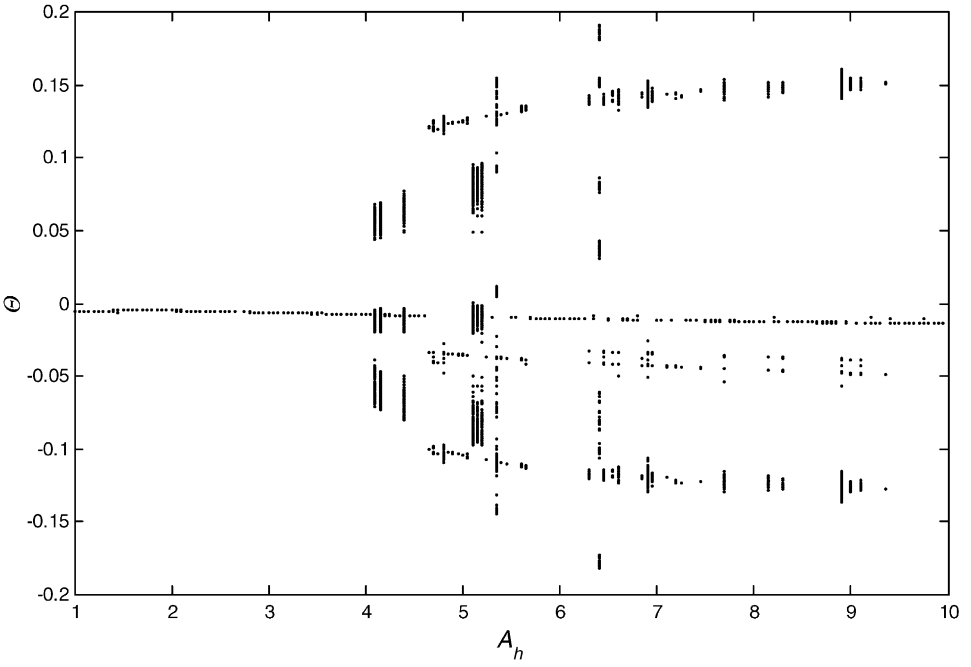

Fig. 11. Change of bifurcation diagram by sliding ($\Omega_h = 10.0$, $\mu_s = \bar{\mu}_s = 0.35$, $\mu_k = \bar{\mu}_k = 0.3$, $e = 0.912$).

on initial conditions and the response can rapidly become chaotic if particular initial conditions are applied. Also, it can be shown that $\frac{1}{3}$ subharmonic response does exist for the case with sliding, but they correspond to different sets of static and dynamic sliding coefficients (see example, Fig. 13).

5.2. Horizontal and vertical excitations

To investigate the effects of sliding motion on the rocking response behavior, system responses corresponding to the bifurcation diagram shown in Fig. 9b (the no sliding case with parameters $\Omega_h = \Omega_v = 10$, $A_h = 3$, $A_v = 0-3$) are simulated with sliding permitted. The resulting bifurcation diagram of the rocking response for the case with static friction coefficient $\mu_s = \bar{\mu}_s = 0.35$ and kinetic friction coefficient $\mu_k = \bar{\mu}_k = 0.3$ (the upper bar means the friction coefficient at impact) is shown in Fig. 14. Comparing with the no sliding case (Fig. 9b), it is observed that the initiation of bifurcation remains unchanged (at $A_v = 1.7$). The transition from $\frac{1}{2}$ to chaotic response initiates at a lower value (A_v about 2.0 instead of 2.3). The range of amplitudes for chaotic response is small compared to the no sliding case and no overturning occurs. This reduction in amplitude is caused by the "base isolation" effect and energy dissipation due to sliding. Fig. 15 shows the time histories of the normalized angular displacement, the normalized horizontal sliding displacement, power spectral density and Poincaré section of an example rocking response

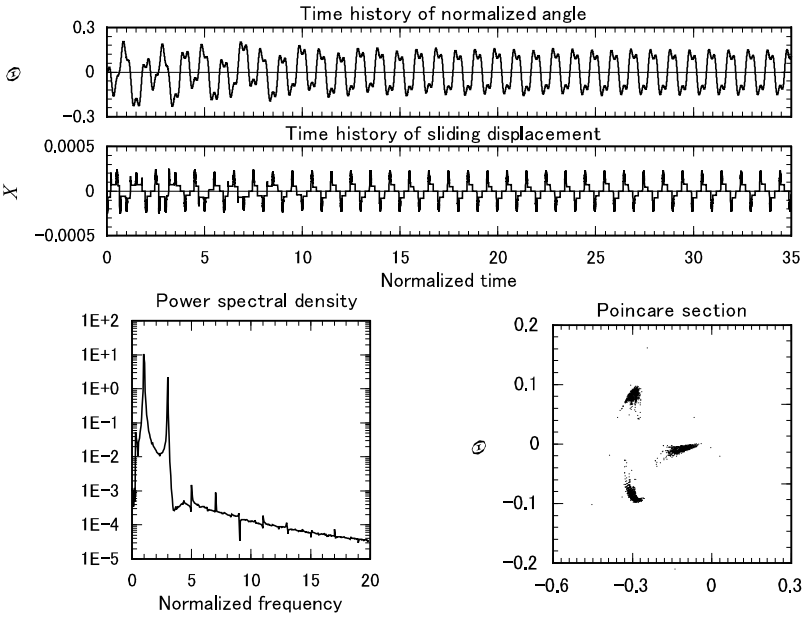

Fig. 12. Effect of sliding on damped rocking response ($\Omega_h = 10.0$, $A_h = 5.2$, $\mu_s = \bar{\mu}_s = 0.35$, $\mu_k = \bar{\mu}_k = 0.3$, $e = 0.912$).

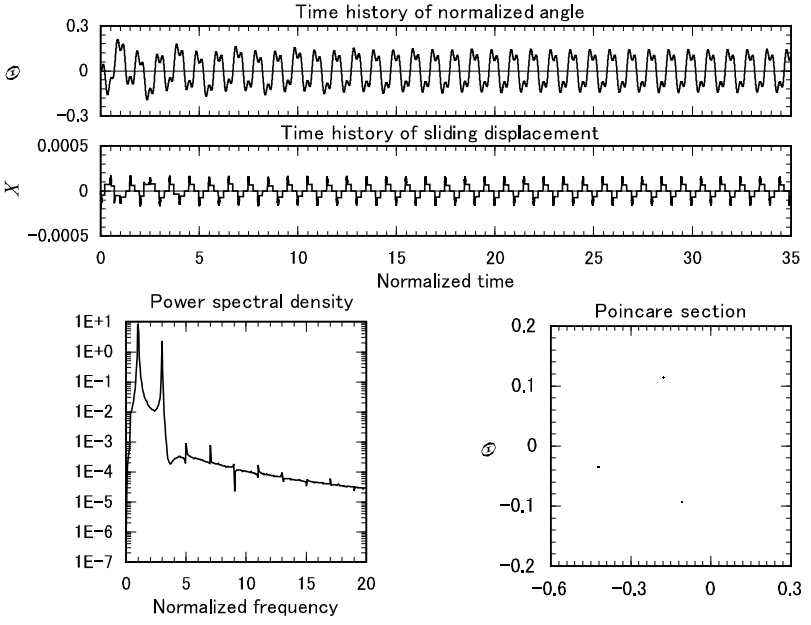

Fig. 13. Example of a damped rocking response with sliding ($\Omega_h = 10.0$, $A_h = 5.2$, $\mu_s = \bar{\mu}_s = 0.4$, $\mu_k = \bar{\mu}_k = 0.35$, $e = 0.912$).

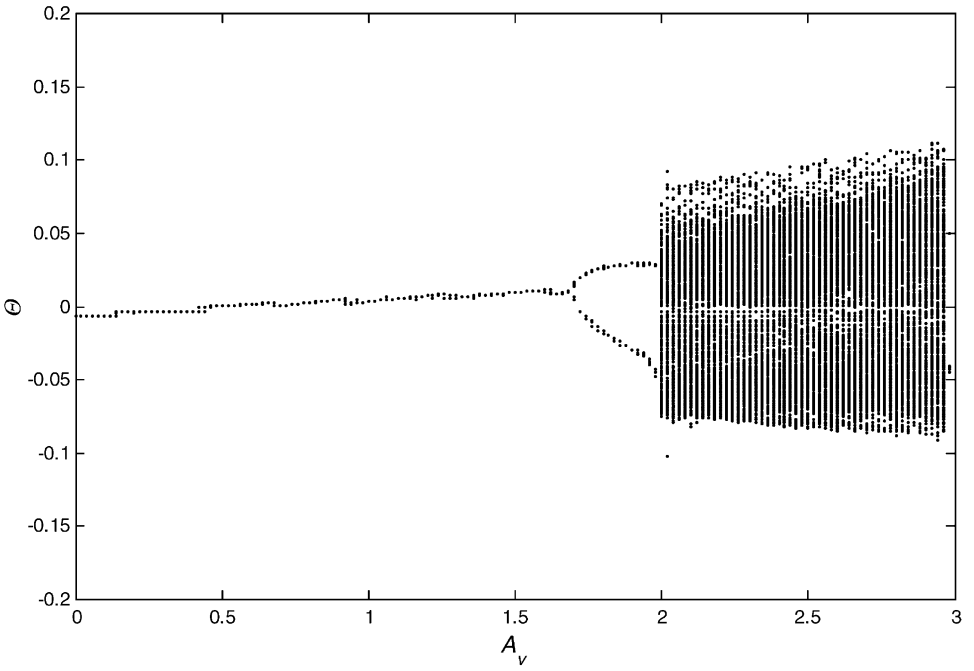

Fig. 14. Bifurcation diagram of rocking response with sliding ($\Omega_h = \Omega_v = 10.0$, $A_h = 3.0$, $\mu_s = \bar{\mu}_s = 0.35$, $\mu_k = \bar{\mu}_k = 0.3$, $e = 0.912$).

with sliding. In the case of no sliding, as shown in Fig. 9b, the rocking response is a $\frac{1}{2}$ subharmonic. However, with sliding, the response becomes chaotic, but with a much smaller response amplitude. Note that sliding is always positive in the case, indicating movement consistently in one direction. Another chaotic response example is shown in Fig. 16, which has exactly the same system and excitation parameters as those shown in Fig. 10, except that sliding is permitted in this case. Note that sliding occurs frequently and in one direction only, and the rocking response amplitude is reduced significantly (see the time history and the Poincaré section, Fig. 16a and d, respectively). Again, this is due to the "base isolation" effect and energy dissipation caused by sliding. Based on our numerical study (not shown here), in the case with sliding, all of the chaotic responses have attractors of similar shape as shown in Fig. 16d. The largest Lyapunov exponent for the response shown in Fig. 16 is 1.76. Compare to the case of no sliding (Fig. 10) the shape of the attractor becomes simpler but the largest Lyapunov exponent increases relatively (from 1.04). Thus, it is observed that the sliding motion intensifies the chaotic behavior of the rocking response and thus the sensitivity to the initial conditions. In the cases examined here, the rocking vibration induced by horizontal and vertical excitations with identical frequency and no phase lag, sliding occurs only in one direction (opposite direction of the excitation during the negative portion). However, based on our numerical study, if the excitation level is sufficiently large, the sliding motion may occur in both the directions of the excitation.

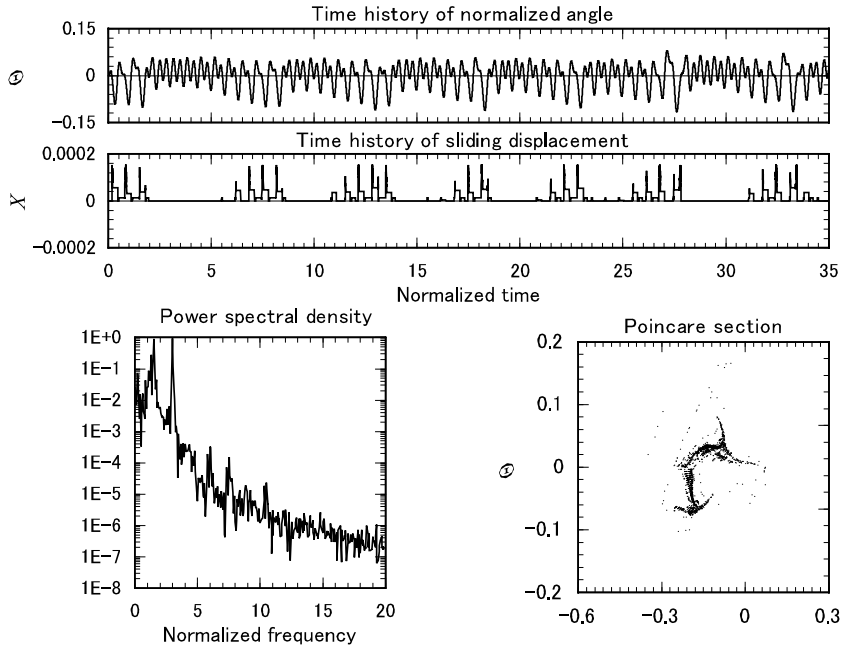

Fig. 15. Damped rocking response under horizontal and vertical excitations with sliding ($\Omega_h = \Omega_v = 10.0$, $A_h = 3.0$, $A_v = 2.0$, $\mu_s = \bar{\mu}_s = 0.35$, $\mu_k = \bar{\mu}_k = 0.3$, $e = 0.912$).

6. Conclusions

In this study, the response characteristics of a rocking rigid object have been examined for both cases of with and without sliding, subjected to horizontal and vertical excitation motions. A response analysis has been carried out, and the conclusions are summarized as follows:

1. The undamped rocking responses subject to horizontal excitation only consist of only quasi-periodic and chaotic motions, thus are sensitive to variations in system and excitation parameters.
2. With the introduction of harmonic excitation in the vertical direction (in addition to the horizontal direction), the quasi-periodic and chaotic responses become even more sensitive to system and excitation parameters.
3. The damped rocking responses to harmonic excitation in the horizontal direction show periodic motions by the effect of the energy dissipation (restitution coefficient e) at impact.
4. In the case without sliding, the region of periodic and quasi-periodic responses is expanded with the increase of excitation frequency. The chaotic region is condensed and number of overturning responses decreases.

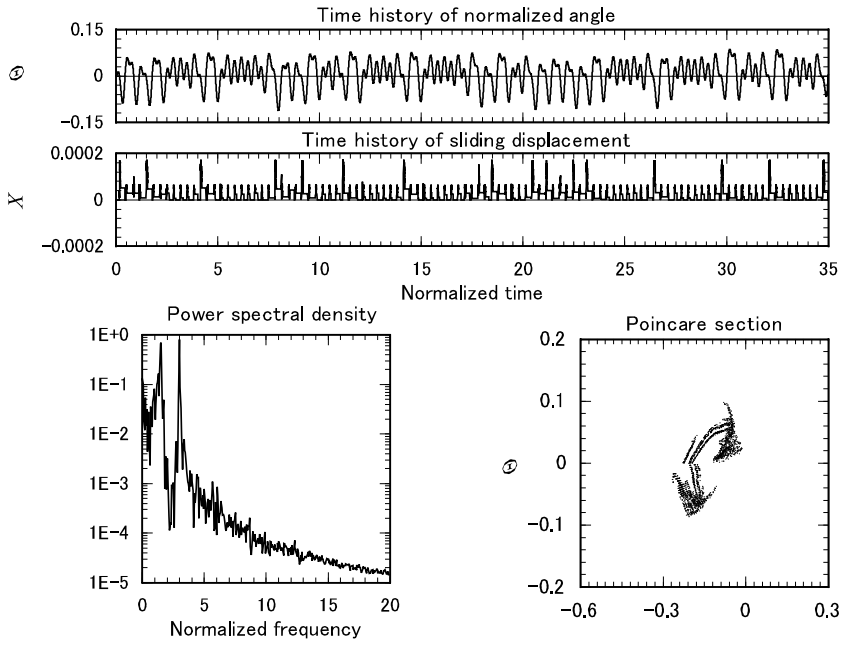

Fig. 16. Effect of sliding on damped rocking response by two-dimensional excitation ($\Omega_h = \Omega_v = 10.0$, $A_h = 3.0$, $A_v = 2.5$, $\mu_s = \bar{\mu}_s = 0.35$, $\mu_k = \bar{\mu}_k = 0.3$, $e = 0.912$).

5. The presence of sliding induces chaotic response in the region which otherwise would have been periodic in the case without sliding. That is, the chaotic response region becomes wider when the sliding motion arises.
6. The occurrence of sliding motion reduces the size of the rocking response chaotic attractor due to energy dissipation caused by the sliding friction. With the lowering of the friction force, the periodic response region becomes narrower and the chaotic response region is expanded.
7. The presence of sliding significantly influences the attractor shape of the rocking response, and the size of the attractor becomes small. The largest Lyapunov exponent is also increased and the chaotic property of the rocking response strengthened.

Acknowledgements

The first author wishes to acknowledge the support from the mechanical dynamics laboratory of Tokyo Metropolitan University for the work presented herein. The third author gratefully acknowledges partial financial support from the Office Naval Research, Grant No. N00014-92-J-1221 and the Civil Engineering Department at Oregon State University.

Appendix A. Algorithm of rocking response analysis program

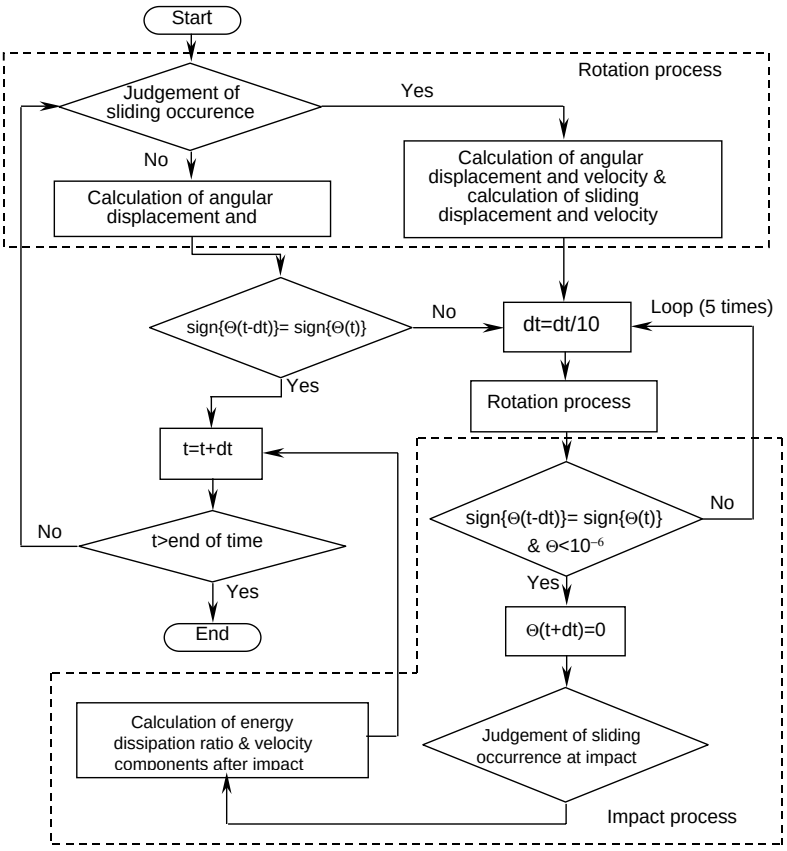

References

[1] S.C.S. Yim, A.K. Chopra, J. Penzien, Rocking response of rigid objects to earthquakes, Earthquake & Engineering Structure Dynamics 8 (6) (1980) 565–587.
[2] M. Aslam, W.G. Godden, D.T. Scalise, Earthquake rocking response of rigid bodies, Journal of Engineering Structure, American Society of Civil Engineers 106 (2) (1980) 377–392.
[3] P.D. Spanos, A.S. Koh, Rocking of rigid blocks due to harmonic shaking, Journal of Engineering Mechanics, American Society of Civil Engineers 110 (11) (1984) 1627–1642.
[4] W.K. Tso, C.M. Wong, Steady state rocking response of rigid blocks Part I: analysis, Earthquake & Engineering Structure Dynamics 18 (106) (1989) 89–106.
[5] S.C.S. Yim, H. Lin, Nonlinear impact and chaotic response of slender rocking objects, Journal of Engineering Mechanics, American Society of Civil Engineers 117 (9) (1991) 2079–2100.
[6] H. Lin, S.C.S. Yim, Nonlinear rocking motions: stability under periodic excitations, Journal of Engineering Mechanics, American Society of Civil Engineers 122 (8) (1996) 719–727.

[7] H. Lin, S.C.S. Yim, Nonlinear rocking motions: overturning under random excitations, Journal of Engineering Mechanics, American Society of Civil Engineers 122 (8) (1996) 728–735.
[8] H.W. Shenton, N.P. Jones, Base excitation of rigid bodies: formulation, Journal of Engineering Mechanics, American Society of Civil Engineers 117 (10) (1991) 2286–2306.
[9] M.Y. Jeong, K. Suzuki, A basic study on the dynamic behavior of rocking rigid body structure, Asia-Pacific Vibration Conference '95, Vol. 95-1, 1995, pp. 365–370.
[10] M.Y. Jeong, K. Suzuki, Experimental investigation of rocking vibration characteristics by two-dimensional excitation, The 74th JSME Spring Annual Meeting, Vol. 74 (4), 1997, pp. 124–127.
[11] M.Y. Jeong, K. Suzuki, A study on the dynamic behavior of rocking rigid body using nonlinear rocking model, Pressure Vessels & Piping Division Conference '97, Vol. 97-4, 1997, pp. 27–34.